

GW150914: Spin based constraints on the merger time of the progenitor system

Doron Kushnir,^{1,2*} Matias Zaldarriaga,¹ Juna A. Kollmeier^{1,3} and Roni Waldman⁴

¹*School of Natural Sciences, Institute for Advanced Study, Princeton, New Jersey, 08540, USA*

²*John N. Bahcall Fellow*

³*Observatories of the Carnegie Institution of Washington, 813 Santa Barbara Street, Pasadena, CA 91101*

⁴*Racah Institute of Physics, Hebrew University, Jerusalem, Israel*

Accepted XXX. Received YYY; in original form ZZZ

ABSTRACT

We explore the implications of the observed low spin of GW150914 within the context of stellar astrophysics and progenitor models. We conclude that many of the recently proposed scenarios are in marked tension with this observation. If the progenitor system was a field binary composed of a black hole (BH) and a Wolf-Rayet star this observation allows us to place a lower limit for the delay time between the formation of the BH+BH binary and the actual merger, $t_{\text{merge}} \gtrsim 10^8$ yr. We anticipate the next series of events, and the associated spin parameters, will ultimately yield critical constraints on formation scenarios and on stellar parameters describing the late-stage evolution of massive stars.

Key words: gravitational waves – binaries: close – stars: Wolf-Rayet

1 INTRODUCTION

The era of gravitational wave astronomy has arrived. Both the strength of the signal in GW150914, as well as its form, were a striking revelation to all (Abbott et al. 2016). In particular, the reported masses of the system — consistent with a black-hole+black-hole (BH+BH) binary merger with estimated BH masses¹ of $M_1 = 35.7^{+5.4}_{-3.8} \pm 1.1$, $M_2 = 29.1^{+3.8}_{-4.4} \pm 0.2$ — are significantly “heavier” than expected based on the known mass function of stellar mass black holes within the Milky Way. The delightfully unexpected properties of GW150914 have unleashed the creative fury of the theoretical astrophysics community. As a result, there is an enormous range of proposed channels all aiming to produce black holes in the observed mass range.

In this article, we explore another property of GW150914 — its observed (low) spin. The effective inspiral spin parameter,

$$\chi_{\text{eff}} = \frac{M_1 \vec{a}_1 + M_2 \vec{a}_2}{M_1 + M_2} \cdot \hat{L} \quad (1)$$

(where \vec{a}_1 and \vec{a}_2 are the dimensionless BH spins, $\vec{a} = c\vec{S}/GM^2$, and \hat{L} is the direction of orbital angular momentum), is observed to be $\chi_{\text{eff}} = -0.06^{+0.17}_{-0.18} \pm 0.01$.

* E-mail: kushnir@ias.edu

¹ The error quotes both the 90% credible interval and an estimate for the 90% range of systematic error (The LIGO Scientific Collaboration & the Virgo Collaboration 2016).

There are multiple proposed channels for the merger of stellar-mass BHs including, but not limited to: isolated stellar field binary merger (hereafter, the *classical scenario*, Phinney 1991; Tutukov & Yungelson 1993; Belczynski et al. 2016), dynamical formation in dense environments (e.g. in globular clusters, Sigurdsson & Hernquist 1993), and merger inside a massive star envelope (Fryer et al. 2001; Reisswig et al. 2013; Loeb 2016; Woosley 2016). Recently, an isolated stellar field binary scenario that includes chemically homogeneous stars has been discussed by Mandel & de Mink (2016); Marchant et al. (2016); de Mink & Mandel (2016). For a more complete reference list of proposed channels see Abbott et al. (2016). Some of these scenarios predict alignment of the BH spin and the orbital angular momentum. In this case χ_{eff} is just the mass-weighted mean of the dimensionless spins $a = c|\vec{S}|/GM^2$, which can generically be quite large in possible tension with the observed low χ_{eff} . For example:

(i) Formation inside a massive star envelope: Reisswig et al. (2013) simulate the fission to two BHs within a common envelope and the subsequent BH-BH merger. In the final orbits before the merger, each BH has $a \approx 0.7$, which would lead to $\chi_{\text{eff}} \approx 0.7$ compared to the low observed value $\chi_{\text{eff}} \ll 1$.

(ii) The chemically homogeneous stars scenario: Yoon et al. (2006) derived the condition $v_{\text{eq}} \geq 0.2\sqrt{GM/R}$, where $v_{\text{eq}} = R\Omega$ is the equatorial velocity at the stellar radius, R , and Ω is the angular spin velocity of the star, as the threshold for homogenous evolution (see their Figure 3;

larger v_{eq} are required for lower mass stars). Neglecting the effect of mass-loss during the collapse of a fully mixed star to a BH (which is justified later on), the dimensionless spin of the BH satisfies:

$$\begin{aligned} a &\geq 0.2cr_g^2\sqrt{\frac{R}{GM}} \\ &\approx 2.7\left(\frac{r_g^2}{0.075}\right)\left(\frac{R}{2R_\odot}\right)^{1/2}\left(\frac{M}{30M_\odot}\right)^{-1/2}, \end{aligned} \quad (2)$$

where r_g^2 is the (dimensionless) radius of gyration of the star related to the moment of inertia by $I = r_g^2 R^2 M$. Equation (2) implies that both BHs should have close to maximal spins ($a \approx 1$). This prediction of $\chi_{\text{eff}} \approx 1$ is thus in seeming tension with the low observed value $\chi_{\text{eff}} \ll 1$. Marchant et al. (2016) provide the a values for their models directly. All systems with $M_1 + M_2 \lesssim 100M_\odot$ that merge within Hubble time satisfy $a \gtrsim 0.5$ for both components, leading to $\chi_{\text{eff}} \gtrsim 0.5$, which also in tension with the low observed value $\chi_{\text{eff}} \ll 1$.

(iii) Perna et al. (2016) suggested that a disk forms around one of the BHs to later power a short gamma-ray burst. The spin of this BH is predicted to be $a \approx 1$ which is also in tension with the low observed value $\chi_{\text{eff}} \ll 1$ for GW150914.

These models, in their raw form, generally predict χ_{eff} close to unity. The observation in GW150914 of $\chi_{\text{eff}} \ll 1$ thus already provides some constraining power on the details of these models.

In this paper we will analyze the *classical scenario* and show that the spin observation allows us to place a lower limit on the delay time between the formation of the BH+BH binary and the actual merger, $t_{\text{merge}} \gtrsim 10^8$ yr. This arises because a short delay time corresponds to small separation between the primary BH and the star that evolves to become the second BH. For small separations, the primary BH applies torque to the star, spinning it towards synchronization. The angular momentum resulting from this process violates the observed upper limit given by the observed χ_{eff} . We elucidate the basic considerations here so that future events may be similarly used to constrain models.

Our paper is organized as follows. In Section 2 we consider the angular momentum evolution of the secondary star as it collapses to a BH, examining the competing effects of wind-losses and torque-gains. In Section 3 we consider the allowed range of scenarios and demonstrate the application of our limits. In Section 4, we consider the caveats and limitations to our main argument. We conclude in Section 5.

2 ANGULAR MOMENTUM EVOLUTION IN A “CLASSIC” SCENARIO

The *classical scenario* for the merger of stellar-mass BHs from an isolated stellar field binary was worked out nearly three decades ago with subsequent modern improvements (Phinney 1991; Tutukov & Yungelson 1993; Belczynski et al. 2016). In this picture, prior to the collapse of the second BH, the progenitor system is an isolated stellar field binary that is composed of a Wolf-Rayet (WR) star with a mass M and a BH with a mass M/q , q being defined as the mass ratio.

We now investigate the angular momentum evolution of the WR star. The final angular momentum of the WR star is the angular momentum of the second BH under the assumption that there is no mass loss during the collapse. We will revisit this assumption in Section 5 and show that mass loss during the collapse does not change our result significantly. We further assume that the kick velocity of the second BH at birth is very small compared with the orbital velocity. Any scenario involving a large BH natal kick is ruled out by the existence of the merger.

For an initial orbital semi-major axis, d , we can normalize the dimensionless spin of the star, a , to the orbital angular velocity, $\omega = \sqrt{G(M+M/q)/d^3}$:

$$\begin{aligned} a &= \frac{cJ}{GM^2} = \frac{cr_g^2 R^2}{GM} \left(\frac{1+q}{2q}\right)^{1/2} \left(\frac{2GM}{d^3}\right)^{1/2} \frac{\Omega}{\omega} \\ &\equiv a_{\text{sync}} \frac{\Omega}{\omega}. \end{aligned} \quad (3)$$

For synchronization between the stellar spin and the orbit ($\Omega = \omega$) we define $a = a_{\text{sync}}$.

Because the merger time due to gravitational wave emission, t_{merge} , also depends simply on the initial orbital properties and component masses (Peters 1964):

$$t_{\text{merge}} = \frac{5}{512} \frac{c^5}{G^3 M^3} \frac{2q^2}{1+q} d^4, \quad (4)$$

we can write a_{sync} as follows:

$$\begin{aligned} a_{\text{sync}} &\approx 0.44 \left(\frac{q^2(1+q)}{2}\right)^{1/8} \left(\frac{r_g^2}{0.075}\right) \left(\frac{R}{2R_\odot}\right)^2 \times \\ &\quad \left(\frac{M}{30M_\odot}\right)^{-13/8} \left(\frac{t_{\text{merge}}}{1\text{Gyr}}\right)^{-3/8}. \end{aligned} \quad (5)$$

It is useful to derive similar expression for the the initial orbital period, equatorial velocity and the break-up fraction:

$$\begin{aligned} P &\approx 1.81 \left(\frac{q^2(1+q)}{2}\right)^{-1/8} \left(\frac{M}{30M_\odot}\right)^{5/8} \left(\frac{t_{\text{merge}}}{1\text{Gyr}}\right)^{3/8} \text{day}, \\ v_{\text{eq}} &= R\Omega = R \left(\frac{1+q}{2q}\right)^{1/2} \left(\frac{2GM}{d^3}\right)^{1/2} \frac{\Omega}{\omega} \\ &\approx 55.8 \left(\frac{q^2(1+q)}{2}\right)^{1/8} \left(\frac{R}{2R_\odot}\right) \times \\ &\quad \left(\frac{M}{30M_\odot}\right)^{-5/8} \left(\frac{t_{\text{merge}}}{1\text{Gyr}}\right)^{-3/8} \frac{\Omega}{\omega} \text{km s}^{-1}, \\ f_{\text{break}} &= \frac{\Omega^2 R^3}{GM} = 2 \left(\frac{R}{d}\right)^3 \left(\frac{1+q}{2q}\right) \left(\frac{\Omega}{\omega}\right)^2 \\ &\approx 1.09 \cdot 10^{-3} \left(\frac{q^2(1+q)}{2}\right)^{1/4} \left(\frac{R}{2R_\odot}\right)^3 \times \\ &\quad \left(\frac{M}{30M_\odot}\right)^{-9/4} \left(\frac{t_{\text{merge}}}{1\text{Gyr}}\right)^{-3/4} \left(\frac{\Omega}{\omega}\right)^2. \end{aligned} \quad (6)$$

The angular momentum evolution of the WR star is determined by two competing process. Stellar winds decrease the angular momentum of the star (Section 2.1), while torque applied to the star by the BH increases the angular momentum, driving it towards a_{sync} (Section 2.2). We now investigate the impact of each of these processes on the total angular momentum evolution.

2.1 Wind Losses

Mass-loss from WR stars is complicated theoretically and observationally, thus the estimated rates are highly uncertain. A typical estimate is $\approx 10^{-5} M_{\odot} \text{yr}^{-1}$ (see Crowther 2007, and references therein), while Nugis & Lamers (2000) estimate $t_M \equiv M/\dot{M} \approx 10^6 \text{yr}$ independent of mass. An expected dependence of the mass loss rate on metallicity further complicates the estimates (Vink et al. 2001). Here we assume that over the time of the WR phase, t_{WR} , the star does not lose a significant fraction of its mass, i.e. $t_{\text{WR}} \lesssim t_M$. For massive $\gtrsim 10 M_{\odot}$ WR stars, this is a reasonable assumption, as the estimated life time is $t_{\text{WR}} \approx 3 \cdot 10^5 \text{yr}$ (see McClelland & Eldridge 2016, for a recent study), and $t_M \gtrsim 10^6 \text{yr}$. We are interested in t_{wind} , the timescale for loss of angular momentum resulting from winds. For $t_{\text{wind}} \lesssim t_{\text{WR}}$ the angular momentum is exponentially suppressed due to the wind. We now estimate this timescale for the system of interest.

Assuming the stellar radius is constant during the mass loss and that the mass is lost from a spherical shell at the stellar surface, we can write the rate of angular momentum loss as follows (Packet 1981):

$$j = i\Omega = \frac{2\dot{M}R^2\Omega}{3}. \quad (7)$$

We can estimate t_{wind} by taking the ratio between J and \dot{J} ,

$$t_{\text{wind}} \equiv \frac{a}{\dot{a}} \approx \frac{J}{\dot{J}} \approx \frac{3}{2} r_g^2 \frac{M}{\dot{M}} \approx 0.1 \left(\frac{r_g^2}{0.075} \right) t_M. \quad (8)$$

2.2 Torque Gains

The torque applied to a star in a binary system was first calculated by Zahn (1975). In our case we can assume that the normalized apparent frequency of the tide, $s = 2|\omega - \Omega| \sqrt{R^3/GM}$, satisfies $s^{-1} \gg 1$:

$$\begin{aligned} s &< 2\omega \left(\frac{R^3}{GM} \right)^{1/2} = 2^{3/2} \left(\frac{1+q}{2q} \right)^{1/2} \left(\frac{R}{d} \right)^{3/2}, \\ \Rightarrow s^{-1} &\gtrsim 15.2 \left(\frac{q^2(1+q)}{2} \right)^{-1/8} \left(\frac{R}{2R_{\odot}} \right)^{-3/2} \\ &\times \left(\frac{t_{\text{merge}}}{\text{Gyr}} \right)^{3/8} \left(\frac{M}{30M_{\odot}} \right)^{9/8}. \end{aligned} \quad (9)$$

In this case the forced oscillations in the envelope behave like a purely traveling wave. For the case that s^{-1} is small compared with unity, one must further consider the damping of the waves in the envelope, which is not the relevant regime and thus outside the scope of the present paper. We use the following expression for the torque applied to the star by the BH, as further described in Kushnir (2016b):

$$\tau \approx \frac{G(M/q)^2}{r_c} \left(\frac{r_c}{d} \right)^6 \left[\frac{4(\omega - \Omega)^2 r_c^3}{GM_c} \right]^{4/3} \frac{\rho_c}{\bar{\rho}_c} \left(1 - \frac{\rho_c}{\bar{\rho}_c} \right)^2, \quad (10)$$

where ρ is the density, $\bar{\rho}$ is the mean density inside the sphere of radius r , and the subscript c indicates values at the convective core boundary. Given this expression for the torque, the change in a can be computed:

$$\dot{a} = \frac{c}{GM^2} \tau \equiv \frac{a_{\text{sync}}}{t_{\tau}} \left| 1 - \frac{a}{a_{\text{sync}}} \right|^{8/3}, \quad (11)$$

where the relevant time scale is

$$\begin{aligned} t_{\tau} &= a_{\text{sync}} \frac{GM^2}{c\tau(\Omega=0)} \\ &= 2^{-21/6} \left(\frac{512}{5} \right)^{17/8} q^{-1/8} \left(\frac{1+q}{2q} \right)^{31/24} r_g^2 \left(\frac{R}{r_c} \right)^2 \\ &\times \left(\frac{GM}{r_c c^2} \right)^{109/24} \left(\frac{GM_c}{r_c c^2} \right)^{4/3} \left(\frac{\rho_c}{\bar{\rho}_c} \right)^{-1} \left(1 - \frac{\rho_c}{\bar{\rho}_c} \right)^{-2} \\ &\times \left(\frac{ct_{\text{merge}}}{r_c} \right)^{9/8} t_{\text{merge}} \\ &\equiv q^{-1/8} \left(\frac{1+q}{2q} \right)^{31/24} f_{\tau}(t_{\text{merge}}) t_{\text{merge}} \end{aligned} \quad (12)$$

In order to estimate this timescale, we require knowledge of the physical structure (R , r_c , M_c , r_g^2) of the WR star. The timescale is especially sensitive to r_c as it scales with r_c^{-9} , and much less sensitive to the other parameters. Note that t_{τ} scales as $t_{\text{merge}}^{17/8}$, and since we are interested in estimating t_{merge} to an order of a magnitude, it is sufficient to estimate f_{τ} (at some fixed t_{merge}) to factor of a few, which we presently evaluate.

2.3 WR stellar models

The values of R , r_c , M_c , and r_g^2 are challenging to directly observe, due to optically thick stellar winds that obscure the stellar surface, making the interpretation of measurements challenging. It is therefore uncertain to use empirical estimates of these quantities, and we are forced to rely on stellar evolution models to obtain estimates of these parameters.

We construct stellar evolution models using the publicly available package MESA version 6596 (Paxton et al. 2011, 2013, 2015). We aim to cover a wide range of masses during the WR phase ($\approx [5, 32] M_{\odot}$), and for that we select from a set of models having ZAMS masses in the range $[40, 100] M_{\odot}$, metallicities between $[0.01, 1] Z_{\odot}$, and initial rotation between $[0.4, 0.6]$ of breakup. We use the WR model profiles during the epoch where the time to core-collapse is greater than 10^4yr and the stellar radius is smaller than $2R_{\text{SM}}$, where R_{SM} is the WR radius according to Schaerer & Maeder (1992).

In all models, mass loss was determined according to the "Dutch" recipe in MESA, combining the rates from Glebbeek et al. (2009); Nieuwenhuijzen & de Jager (1990); Nugis & Lamers (2000); Vink et al. (2001), with a coefficient $\eta = 1$, convection according to the Ledoux criterion, with mixing length parameter $\alpha_{\text{mlt}} = 2$, semi-convection efficiency parameter $\alpha_{\text{sc}} = 0.1$ (Paxton et al. 2013, eq. 12), and exponential overshoot parameter $f = 0.008$ (Paxton et al. 2011, eq. 2). For the atmosphere boundary condition we use the simple option of MESA (Paxton et al. 2011, eq. 3).

In Figure 1 we present R and r_c a function of M for the models we consider. Our results can be fit as $\log_{10}(R/R_{\odot}) \approx -0.70 + 0.70 \log_{10}(M/M_{\odot})$ and as $\log_{10}(r_c/R_{\odot}) \approx -1.25 + 0.75 \log_{10}(M/M_{\odot})$. The profiles are well described by polytropes with $n \approx 2.5 - 3.5$ and r_g^2 is in the range $\approx 0.05 - 0.09$, which roughly corresponds to these polytropes. Our calculated stellar radii are compared with the stellar evolution models of Schaller et al. (1992), evaluated in Schaerer & Maeder (1992). We predict larger radii ($\sim 30\%$) at fixed mass in our models relative to the Schaller et al.

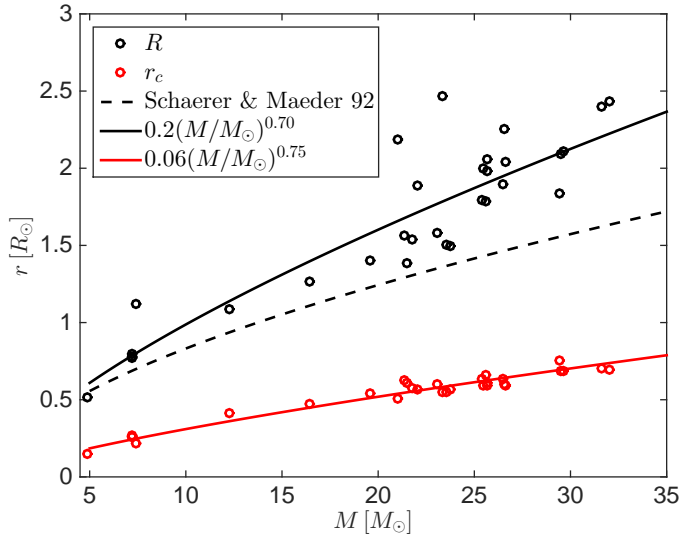


Figure 1. R (black curves) and r_c (red curves) for a series of stellar models. The open symbols show our results for a series of models computed by MESA. Simple fits to these points are shown by the solid black and red curves. The dashed black curve shows the estimate of R from Schaefer & Maeder (1992) based on the stellar evolution models of Schaller et al. (1992). The predicted larger radii ($\sim 30\%$) at fixed mass in our models relative to the Schaller et al. (1992) models, likely due to our simplified treatment of the stellar atmosphere, do not significantly impact our final results.

(1992), possibly because of the simple MESA photosphere boundary condition that we used. We note that generally, stellar evolution models predict radii that are significantly smaller than those derived from atmospheric models ($\approx 3R_\odot$ in some cases; see Crowther 2007, and references therein), and therefore should be considered at the moment as a rough estimate. Nevertheless, the uncertainty in the stellar radii is insignificant for our final results, which depend much more strongly on the core radii.

Instead of fitting separately for each parameter, we directly calculate, for each WR model, $f_\tau(1\text{Gyr})$ from Equation (12). The results are presented in Figure 2. The main uncertainty in the value of f_τ is the core radius r_c , as $f_\tau \propto r_c^{-9}$. The scatter of f_τ at fixed mass is completely driven by the scatter of r_c in Figure 1. We approximate $f_\tau(1\text{Gyr}) \approx 2.4 \cdot 10^{-3} (M/10M_\odot)^{1.98}$, which reproduces the numerical results to better than a factor of 3. This allows us to rewrite Equation (12) simply as

$$t_\tau \approx 2.1 \cdot 10^7 q^{-1/8} \left(\frac{1+q}{2q} \right)^{31/24} \left(\frac{M}{30M_\odot} \right)^{1.98} \left(\frac{t_{\text{merge}}}{1\text{Gyr}} \right)^{17/8} \text{ yr.} \quad (13)$$

One can adopt, to nearly the same level of precision, $f_\tau(1\text{Gyr}) \approx 0.01$, which changes our conclusions insignificantly. We are now able to evaluate the angular momentum evolution of the system prior to merger.

3 IMPLICATIONS

At the beginning of the WR phase, we expect $0 \leq a \leq a_{\text{sync}}$. That is, we neither expect the star to be spinning faster than the synchronization value nor retrograde. We can therefore

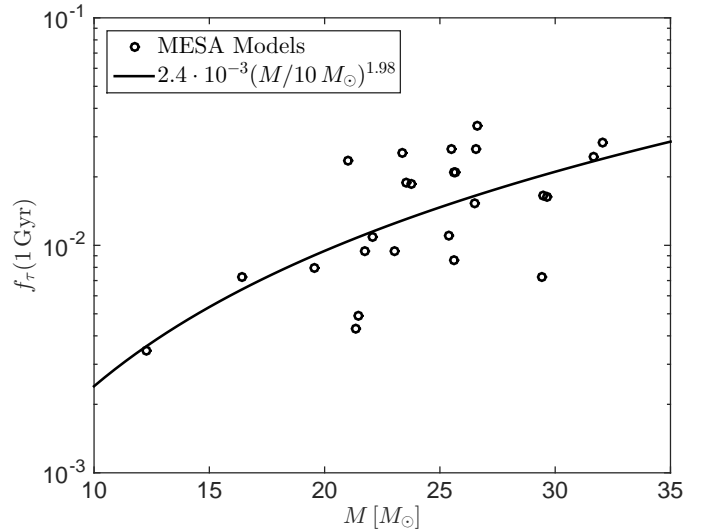


Figure 2. The pre-factor from Equation (12), $f_\tau(1\text{Gyr})$, as function of the stellar mass. The main uncertainty in the value of f_τ is the core radius r_c , as $f_\tau \propto r_c^{-9}$. The scatter of f_τ at fixed mass is completely driven by the scatter of r_c in Figure 1. We approximate $f_\tau(1\text{Gyr}) \approx 2.4 \cdot 10^{-3} (M/10M_\odot)^{1.98}$, which reproduces the numerical results to better than a factor of 3. One can also take a constant value for f_τ , $f_\tau(1\text{Gyr}) \approx 0.01$, without changing our conclusions significantly.

compute the evolution of the spin taking into account the breaking and torquing described above. Including both effects, the evolution of a is simply

$$\dot{a} = \frac{a_{\text{sync}}}{t_\tau} \left(1 - \frac{a}{a_{\text{sync}}} \right)^{8/3} - \frac{a}{t_{\text{wind}}}, \quad (14)$$

We can integrate Equation (14) directly to find $a(t_{\text{WR}})$ given t_{WR} , t_{wind} , t_τ , and $a(0)$. The angular momentum of the second BH is given by $\min(a(t_{\text{WR}}), 1)$.

We solve Equation (14) for four representative examples and show the results in Figure 3. We consider cases when $t_{\text{wind}} \gtrsim t_{\text{WR}}$ or $t_{\text{wind}} \lesssim t_{\text{WR}}$ and when the initial spin is close to zero or close to a_{sync} . In our examples for Figure 3 we choose $t_{\text{WR}}/t_{\text{wind}} = 0.3$ and $t_{\text{WR}}/t_{\text{wind}} = 3$ so as to span reasonable parameters for the wind. We further assume that $q = 1$, consistent with GW150914. Our results are compared with the limit from GW150914, $a < 0.3$ at 90% probability (The LIGO Scientific Collaboration & the Virgo Collaboration 2016). In our comparison, we use the values for the less massive BH as the more massive BH yields slightly stronger constraints. We conclude that in order for a not to exceed the observed limit, we must have $t_{\text{merge}} \gtrsim 10^8 \text{ yr}$. For example, the vast majority of models in (Belczynski et al. 2016) fulfill this condition. Note that the scenario of no winds and $a(0) = a_{\text{sync}}$ is not far from being ruled out, as using the age of the Universe for t_{merge} in Equation (3) leads in this case to $a = a_{\text{sync}} \approx 0.15$.

4 CAVEATS

We assume there is no mass loss during the collapse. Mass loss changes our analysis in two ways. First, mass loss

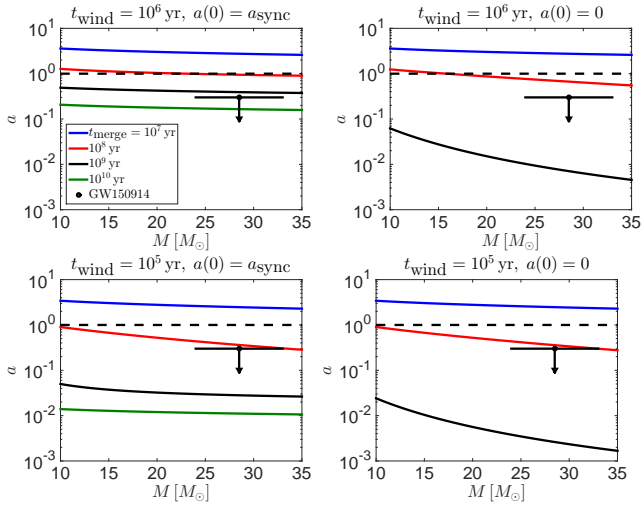


Figure 3. Dimensionless spin-parameter of the secondary BH as a function of M for different limiting cases. The black symbol shows GW150914. Blue, red, black, and green lines show merger times of 10^7 , 10^8 , 10^9 and 10^{10} yr. We choose $t_{\text{WR}}/t_{\text{wind}} = 0.3$ and $t_{\text{WR}}/t_{\text{wind}} = 3$ to span reasonable parameters for the wind. For convenience, we plot values above the $a = 1$ limit (dashed line).

widens the initial separation of the BH+BH orbit compared with the BH+WR orbit. This effect makes the merger time longer, which does not affect the derived lower limit for t_{merge} . Second, angular momentum is lost with the mass ejection, which may change our estimate for the spin evolution of the BH. We estimate the possible decrease in a by considering in Figure 4 polytropes with solid body rotation, which is the expected configuration during the WR phase. The very last burning stages of the WR star prior to collapse are expected to be sufficiently fast, such that angular momentum transfer can be neglected and each mass shell retains its original a value, making this polytrope estimate robust. We show in Figure 4 that the value of a can decrease by 20–40% for a large mass ejection, which does not significantly affect our analysis. Moreover, if indeed the collapse was accompanied by a supernova, then it should be a Type Ibc supernova, for which the mass of the ejecta is small compared to $30M_{\odot}$ (e.g., Lyman et al. 2014). Indeed, such a system is an expected outcome of a Type Ibc supernova for collapse-induced thermonuclear explosions (Kushnir 2015a,b).

We thus conclude that our analysis is robust to the simplifications we have made.

5 DISCUSSION

We have provided a simple framework for using the observed (low) BH spin of GW150914 to constrain the BH merger time and thus the characteristics of the progenitor system. We have shown that already with a single event, the observed constraint on χ_{eff} comes astonishingly close to ruling out certain scenarios. We eagerly await the results of future observations of gravity waves from these truly remarkable events and expect that the measurement of the spins will be very informative to constrain the different formation channels that have been proposed.

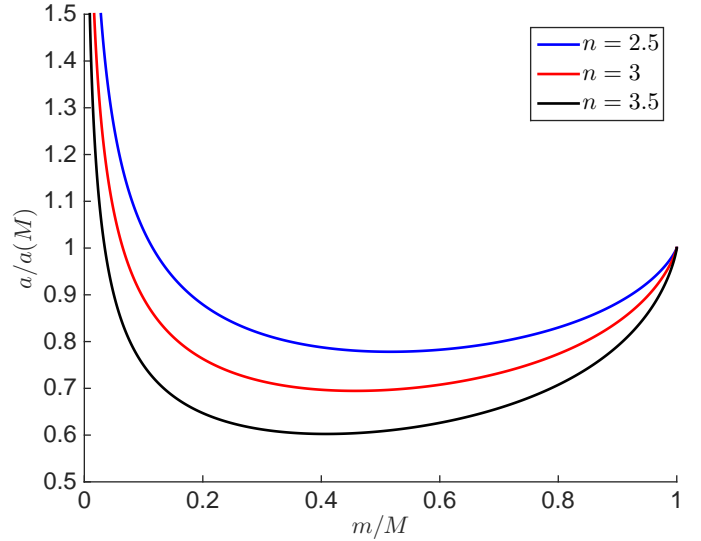


Figure 4. Effect of mass loss on angular momentum evolution. We compute the change in a for three different polytropes in solid-body rotation as mass is changed relative to an initial mass. The possible decrease in a is modest (20–40%), and obtained for substantial mass-loss.

ACKNOWLEDGEMENTS

We thank Ben Bar-Or, Boaz Katz, Roman Rafikov, and Eli Waxman for discussions. M.Z. is supported in part by the NSF grants PHY-1213563, AST-1409709 and PHY-1521097. JAK gratefully acknowledges support from the Institute for Advanced Study.

REFERENCES

- Abbott, B. P., Abbott, R., Abbott, T. D., et al. 2016, *Physical Review Letters*, 116, 061102
- Abbott, B. P., Abbott, R., Abbott, T. D., et al. 2016, *ApJ*, 818, L22
- Belczynski, K., Holz, D. E., Bulik, T., & O’Shaughnessy, R. 2016, arXiv:1602.04531
- Crowther, P. A. 2007, *ARA&A*, 45, 177
- de Mink, S. E., & Mandel, I. 2016, arXiv:1603.02291
- Fryer, C. L., Woosley, S. E., & Heger, A. 2001, *ApJ*, 550, 372
- Glebbeek, E., Gaburov, E., de Mink, S. E., Pols, O. R., & Portegies Zwart, S. F. 2009, *A&A*, 497, 255
- Kushnir, D. 2015a, arXiv:1502.03111
- Kushnir, D. 2015b, arXiv:1506.02655
- Kushnir, D., Zaldarriaga, M., Kollmeier, J.A., Waldman, R. 2016b, arXiv
- The LIGO Scientific Collaboration, & the Virgo Collaboration 2016, arXiv:1602.03840
- Loeb, A. 2016, *ApJ*, 819, L21
- Lyman, J., Bersier, D., James, P., et al. 2014, arXiv:1406.3667
- Mandel, I., & de Mink, S. E. 2016, *MNRAS*, 458, 2634
- Marchant, P., Langer, N., Podsiadlowski, P., Tauris, T. M., & Moriya, T. J. 2016, *A&A*, 588, A50
- McClelland, L. A. S., & Eldridge, J. J. 2016, *MNRAS*
- Nieuwenhuijzen, H., & de Jager, C. 1990, *A&A*, 231, 134
- Nugis, T., & Lamers, H. J. G. L. M. 2000, *A&A*, 360, 227
- Packet, W. 1981, *A&A*, 102, 17
- Paxton, B., Bildsten, L., Dotter, A., et al. 2011, *ApJS*, 192, 3
- Paxton, B., Cantiello, M., Arras, P., et al. 2013, *ApJS*, 208, 4

- Paxton, B., Marchant, P., Schwab, J., et al. 2015, ApJS, 220, 15
Peters, P. C. 1964, Physical Review, 136, 1224
Perna, R., Lazzati, D., & Giacomazzo, B. 2016, arXiv:1602.05140
Phinney, E. S. 1991, ApJ, 380, L17
Reisswig, C., Ott, C. D., Abdikamalov, E., et al. 2013, Physical Review Letters, 111, 151101
Schaerer, D., & Maeder, A. 1992, A&A, 263, 129
Schaller, G., Schaerer, D., Meynet, G., & Maeder, A. 1992, A&AS, 96, 269
Sigurdsson, S., & Hernquist, L. 1993, Nature, 364, 423
Tutukov, A. V., & Yungelson, L. R. 1993, MNRAS, 260, 675
Vink, J. S., de Koter, A., & Lamers, H. J. G. L. M. 2001, A&A, 369, 574
Woosley, S. E. 2016, arXiv:1603.00511
Yoon, S.-C., Langer, N., & Norman, C. 2006, A&A, 460, 199
Zahn, J.-P. 1975, A&A, 41, 329

This paper has been typeset from a $\text{\TeX}/\text{\LaTeX}$ file prepared by the author.